New Phytologist

Research

MicroRNA399s and strigolactones mediate systemic phosphate signaling between dodder-connected host plants and control association of host plants with rhizosphere microbes

Man Zhao[1,2], Xijie Zheng[1,2], Zhongxiang Su[1], Guojing Shen[1,2], Yuxing Xu[1,2], Zerui Feng[1,2], Wenxing Li[1,2], Shuhan Zhang[1,2], Guoyan Cao[1,2], Jingxiong Zhang[1,2] and Jianqiang Wu[1,2,3]

[1]Department of Economic Plants and Biotechnology, Yunnan Key Laboratory for Wild Plant Resources, Kunming Institute of Botany, Chinese Academy of Sciences, Kunming, 650201, China; [2]CAS Center for Excellence in Biotic Interactions, University of Chinese Academy of Sciences, Beijing, 100049, China; [3]State Key Laboratory of Plant Diversity and Specialty Crops, Beijing, 100093, China

Authors for correspondence:
Jianqiang Wu
Email: wujianqiang@mail.kib.ac.cn

Jingxiong Zhang
Email: zhangjingxiong@mail.kib.ac.cn

Received: *1 June 2024*
Accepted: *24 October 2024*

New Phytologist (2025) **245:** 1263–1276
doi: 10.1111/nph.20266

Key words: AMF, dodder, microRNA399, phosphate starvation, rhizosphere bacterial community, strigolactones, systemic signaling.

Summary

- A dodder (*Cuscuta*) often simultaneously parasitizes two or more adjacent hosts. Phosphate (Pi) deficiency is a common stress for plants, and plants often interact with soil microbes, including arbuscular mycorrhizal fungi (AMF), to cope with Pi stress. Little is known about whether dodder transmits Pi deficiency-induced systemic signals between different hosts.
- In this study, dodder-connected plant clusters, each composed of two tobacco (*Nicotiana tabacum*) plants connected by a dodder, were established, and in each cluster, one of the two tobacco plants was treated with Pi starvation. AMF colonization efficiency, rhizosphere bacterial community, and transcriptome were analyzed in the other dodder-connected Pi-replete tobacco plant to study the functions of interplant Pi signals.
- We found that dodder transfers Pi starvation-induced systemic signals between host plants, resulting in enhanced AMF colonization, changes of rhizosphere bacterial communities, and alteration of transcriptomes in the roots of Pi-replete plants. Importantly, genetic analyses indicated that microRNA399s (miR399s) and strigolactones suppress the systemic Pi signals and negatively affect AMF colonization in the Pi-replete plants.
- These findings provide new insight into the ecological role of dodder in mediating host–host and host–microbe interactions and highlight the importance of strigolactone and miR399 pathways in systemic Pi signaling.

Introduction

Parasitism and mutualism are very common forms of interaction in nature. Approximately 1% of angiosperms, which evolved from 12 or 13 origins, are parasitic plants (Westwood *et al.*, 2010; Nickrent, 2020). Through an organ named haustorium, these parasites obtain nutrients and water from their host plants to sustain growth and development. Dodders (*Cuscuta* spp., Convolvulaceae) are obligate holoparasitic/nearly holoparasitic plants that parasitize on stems of host plants across various families. Dodders are leafless and rootless, and through haustoria, they extract nutrients and water from hosts (Yoshida *et al.*, 2016). Dodder stems slowly rotate, and when touching adjacent neighboring plants, they twine around neighboring plants and often establish parasitism. Thus, a dodder plant can parasitize on more than one host simultaneously, forming a network of interconnected plants known as a dodder-connected plant cluster (Hettenhausen *et al.*, 2017).

The connections between dodder and host vasculature via haustoria form important pathways for transmission of various biomolecules between dodder and hosts and among dodder-connected hosts (Yoshida *et al.*, 2016; Shen *et al.*, 2023). Increasing lines of evidence have shown that macromolecules, including mRNAs (Kim *et al.*, 2014; Song *et al.*, 2022), microRNAs (Shahid *et al.*, 2018), and proteins (Liu *et al.*, 2020; Shen *et al.*, 2020), are transferred between dodder and host plants or even between dodder-connected host plants. Importantly, through dodder bridge connections, systemic signals can be transferred from one host to another, where the systemic signals activate defense- or stress adaptation-related physiological responses (Shen *et al.*, 2023). The physiological and ecological functions of dodder-transmitted between-plant signaling remain poorly understood.

Phosphorous (P) is a crucial macromineral element for plant growth and development. Inorganic phosphate (Pi) is the main form of P that can be taken up directly by plants (López-Arredondo *et al.*, 2014). Due to the low availability and poor mobility of Pi in the soil, the plant rhizosphere quickly forms Pi-depleted zones. To adapt to low-Pi conditions, plants have evolved elaborate strategies collectively known as Pi starvation

responses (PSRs) (Thibaud *et al.*, 2010). PSRs include increased density of root hairs and altered expression of genes involved in Pi uptake and transport (Lambers, 2022). Systemic signaling is essential in PSRs as well. Different parts of a root often experience different Pi contents in soil, and systemic signaling coordinates PSRs in different root parts. Split-root experiments showed that systemic signals are transferred between the Pi-starved root part and Pi-replete root part of *Brassica napus* (Li *et al.*, 2022). A conserved small RNA microRNA399 (miR399) family, which is systemically transmitted between root and shoot, plays an important role in regulating PSRs and Pi homeostasis (Pant *et al.*, 2008; Chien *et al.*, 2018). The levels of miR399s are positively regulated by the transcription factor PHR1 (phosphate starvation response 1), and miR399s are highly accumulated in phloem sap under Pi-deficiency conditions. miR399s can be transported from shoot to root to activate degradation of the target gene *PHOSPHATE 2* (*PHO2*), which encodes a ubiquitin-conjugating E2 enzyme (Aung *et al.*, 2006; Bari *et al.*, 2006). PHR1 also regulates a nonprotein-coding gene *IPS1* (*INDUCED BY PHOSPHATE STARVATION 1*), which inhibits miR399-mediated degradation of *PHO2* mRNA by a target mimicry mechanism (Franco-Zorrilla *et al.*, 2007).

An important strategy for plants to obtain P is to interact with rhizosphere microorganisms including arbuscular mycorrhizal fungi (AMF) and bacteria (Wang *et al.*, 2022; Zhao *et al.*, 2023). AMF access large ranges of soil through extensive extracellular mycelia (ERM) (Nussaume *et al.*, 2011), and together with the P-solubilizing bacteria, which colonize the ERM and decompose organic and nonsoluble inorganic P, ERM transfer Pi to plants (Wang *et al.*, 2022; Duan *et al.*, 2023; Shi *et al.*, 2023). In return, plants provide AMF with lipids and sugars (Jiang *et al.*, 2017; Bennett & Groten, 2022). The symbiosis between plants and AMF is controlled by the PHR-regulated network regulated by exogenous P conditions and endogenous P sensing mechanisms (Shi *et al.*, 2021). Strigolactones (SLs) play an important role in regulating plant growth and development. β-Carotenoids are converted to SLs by a series of enzymes, among which carotenoid cleavage dioxygenase 8 (CCD8) is one of the key enzymes (Alder *et al.*, 2012). The SL pathway is important for plant adaptation to low-Pi stress. Under the conditions of low-soil Pi, the biosynthesis of SLs is activated (Das *et al.*, 2022; Barbier *et al.*, 2023) and plants secrete SLs into rhizosphere to promote symbiosis with soil microorganisms, including AMF (Siddiqi & Husen, 2017).

A dodder parasite often bridge connects two or multiple hosts simultaneously. Yet little is known about whether and how dodder parasites transmit different interplant systemic signals induced by environmental stresses and developmental cues. Given the involvement of long-distance Pi signaling in PSRs (Chiou & Lin, 2011), we hypothesized that in dodder-connected plant clusters, when one plant suffers from Pi starvation, dodder may transfer systemic signals to the other dodder-connected host plant, where the systemic signals regulate the symbiosis of the other host with AMF and affect the rhizosphere bacterial community. In this study, a tobacco (*Nicotiana tabacum*)-dodder (*Cuscuta campestris*)-tobacco parasitization system was used to examine this hypothesis. Genetic analyses were done to study the functions of SL and miR399 pathways in such a dodder-mediated plant–plant interaction system.

Materials and Methods

Plant materials

Dodder (*Cuscuta campestris* Yunck.) seeds were germinated using a previously published method by Zhang *et al.* (2024). Dodder seedlings were used to parasitize the wild tomato (*Solanum pennellii* Correll), forming dodder stocks. Tobacco (*Nicotiana tabacum* L.) seeds were surface sterilized with 10% sodium hypochlorite for 10 min and washed five times with sterile water, before being sown in sterilized nutrient soil (PINDSTRUP, https://www.pindstrup.com). Cucumber (*Cucumis sativus* L.) seeds were germinated on moist filter paper. All the plants were cultivated in a glasshouse under a condition of 16 h : 8 h, 25°C : 18°C, light : dark photoperiod.

The methods for obtaining transgenic plants of oeIPS1 and *ccd8* are described in Supporting Information Methods S1. The primers used are listed in Table S1.

Preparation of dodder-connected plant clusters, mycorrhizal inoculation, and plant treatments

For tobacco/cucumber-dodder-tobacco experiments, plants seedlings (tobacco/cucumber) designated as the systemic signals donor (SD) plants were transplanted into 1-l plastic pots filled with modified Hoagland solution (MHS, recipe is shown in Table S2) (Zhang *et al.*, 2024). Plants designated as the systemic signals receiver (SR) plants were transplanted into 1-l pots containing sterilized mixture of sand and perlite (3 : 1) and watered with MHS. After 2 wk, vigorously growing dodder stems were excised from stocks and used for infestation of stems of each pair of SD and SR plants. After *c.* 3 wk, dodder successfully parasitized each pair of SD and SR plants, forming bridge connections between these SD plants and SR plants. Only SD and SR plants with similar degrees of dodder infestation were used for further experiments. SR plants were supplemented with 100 ml of sand containing AMF (*Rhizophagus irregularis* (DAOM 197198), *c.* 1000 spores), and the SD plants were supplied with MHS, which contained 1 mM KH_2PO_4 (+P), or MHS without KH_2PO_4 (−P, KH_2PO_4 was replaced with KCl). The SD plants were given fresh MHS (+P or −P) every 3 d. After 18 d, the fifth leaves and part of the roots from the host plants were carefully harvested and frozen in liquid nitrogen and then stored at −80°C for further analysis. The rest of roots were used for AMF colonization assessment.

Colonization efficiency detection

The colonization efficiency was evaluated based on a previously published method (Shi *et al.*, 2021). Tobacco roots were stained with trypan blue, and the colonizing structure was observed by microscope (Leica DM5500 B). The detailed method is described in Methods S1.

Rhizosphere bacterial community analysis in dodder-connected plant clusters

For the rhizosphere bacterial community experiments, SD plants were prepared as above, SR plants were transplanted into 1-l pots containing mixed soil (nutrient soil: perlite: pastoral soil = 5 : 2 : 1), in which the pastoral soil was taken from the Kunming Botanical Garden (N25°8′14″, E102°44′34″, altitude 1930 m). After 3 wk, vigorously growing dodder stems were used to connect each pair of SD plant and SR plant, forming the tobacco-dodder-tobacco clusters. When the clusters were successfully established, the SD plants were given MHS with Pi or without Pi every 3 d. After 18 d, the rhizosphere soil of the SR plants was harvested. The methods used for rhizosphere soil collection and 16S ribosomal RNA (rRNA) profiling are described in Methods S1.

Determination of Pi and total P content

The improved molybdate-blue method was used for detection of Pi contents (Nanamori *et al.*, 2004). The detailed method is described in Methods S1.

For detection of total P content, samples were dried at 105°C for 3 h and 65°C for 72 h, before being ground to fine powder. Samples (100 mg) were digested thoroughly by concentrated H_2SO_4 and H_2O_2 in digestion vessels. The treated samples were then analyzed by continuous flow analyzer (AA3).

Determination of soil phosphatase activity

Soil phosphatase activity was determined using a soil acid phosphatase activity detection kit and a soil alkaline phosphatase activity detection kit (Solarbio, Beijing, China).

RNA isolation and RNA-Seq analysis

For each group, three biological replicates, each of which was pooled from two independent samples, were used for RNA library construction and sequencing. Total RNA was extracted from *c.* 100 mg of samples using the TRIzol reagent (Thermo Fisher, Waltham, CA, USA) following the manufacturer's protocol. The detail can be found in Methods S1.

Relative quantification and sequencing of miR399s and mRNAs

The expression of miR399s was quantified following a stem-loop reverse transcription polymerase chain reaction method (Varkonyi-Gasic *et al.*, 2007). cDNA synthesis was performed following the manufacturer's protocol (TaKaRa, Shiga, Japan, PrimeScript™ RT reagent Kit). The details are described in Methods S1.

Statistical analysis

Statistical analysis was performed using R (v.4.2.1) (https://www.r-project.org). Student's *t*-test was applied for comparisons of two groups. One-way and two-way ANOVA were performed when there were more than two groups. Data are shown as means ± standard deviation.

Results

Systemic signals from Pi deficiency-treated host plants increase AMF colonization in dodder-connected Pi-replete host plants

First, we examined if dodder parasitization could affect AMF colonization in individual host plants. Tobacco plants were either infested with a dodder or kept noninfested. When parasitism was well established, the tobacco plants were inoculated with AMF and treated with Pi starvation or untreated. After 4 wk, the AMF colonization efficiency was measured in these four groups of plants (Fig. S1a). Compared with the corresponding control plants, which were treated with the Pi-replete medium, the Pi-depleted unparasitized and parasitized tobacco plants showed, respectively, 18% and 36% increased AMF colonization efficiency, indicating that dodder-parasitized tobacco plants could still respond to Pi stress by increasing AMF colonization, although dodder parasitism decreased the symbiosis of AMF with tobacco under normal and Pi-stress conditions (Fig. S1b).

Next, we sought to determine in a dodder-connected plant cluster, whether Pi deficiency in one host plant can lead to any physiological changes in the other dodder-connected Pi-replete host plant. We treated the systemic signals donor (SD) tobacco hosts with Pi deficiency (−P) or mock treatment (+P), and the AMF colonization efficiency was quantified in the other systemic signal receiver (SR) tobacco, which was continuously grown under normal nutrient conditions (Pi replete) (Fig. 1a). We found that the AMF colonization efficiency of the SR plants increased 38% when being connected to the −P-treated SD plants by dodder, compared to those being connected to the +P-treated SD plants (Fig. 1b). Furthermore, a similar result was obtained when we used cucumber (*Cucumis sativus*) as the SD plants (Fig. 1c,d). These results suggest that dodder transmitted certain Pi deficiency-induced systemic signals from the SD plants to the SR plants, where the signals promoted symbiosis between the SR plants and AMF, and these signals are likely well conserved among plants of different families.

miR399s and strigolactones in systemic signals donor plants negatively regulate dodder-mediated interplant Pi signaling

Previous studies have revealed that the miR399 and strigolactone (SL) pathway are, respectively, involved in shoot-root systemic Pi signaling and root–AMF interactions (Branscheid *et al.*, 2010; Lanfranco *et al.*, 2018; Santoro *et al.*, 2021). Therefore, we next examined whether the miR399 and SL pathway are required for dodder-mediated interplant Pi signaling.

Both stable transformation in Arabidopsis and transient expression in *Nicotiana benthamiana* indicated that *IPS1* (*INDUCED BY PHOSPHATE STARVATION1*) can block the inhibitory effect of miR399s on the target gene *PHO2* through a target mimicry

New Phytologist

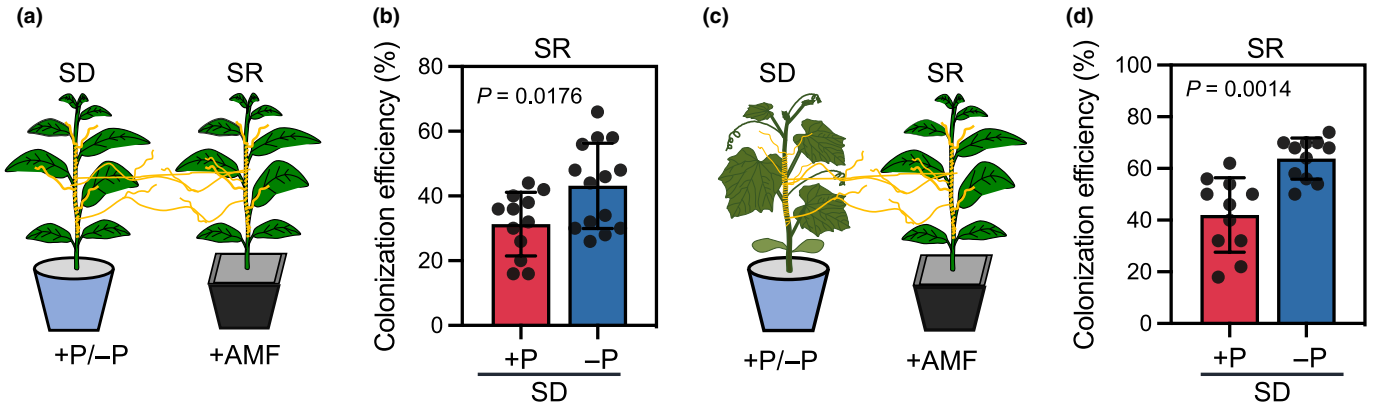

Fig. 1 Arbuscular mycorrhizal fungi (AMF) colonization efficiency in systemic signals receiver plants of dodder-connected tobacco plant clusters. (a, b) In tobacco (*Nicotiana tabacum*)-dodder (*Cuscuta campestris*)-tobacco plant clusters (a), the systemic signals donor (SD) tobacco plants were treated with phosphate (+P) or no phosphate (−P) conditions, and the systemic signals receiver (SR) tobacco plants were inoculated with AMF. After 18 d, AMF colonization efficiencies in the SR plants were measured (b). (c, d) In cucumber (*Cucumis sativus*)-dodder-tobacco plant clusters (c), the SD cucumber plants were treated with phosphate (+P) or no phosphate (−P) conditions, and the SR tobacco plants were inoculated with AMF. After 18 d, AMF colonization efficiencies in the SR plants were measured (d). +P: 1 mM KH_2PO_4, −P: 0 mM KH_2PO_4. Data are mean ± standard deviation; n = 12–14. Student's t-test (P-values are indicated in the graphs).

mechanism (Franco-Zorrilla *et al.*, 2007). Given the high similarities of Arabidopsis miR399s and tobacco nta-miR399s (Lin *et al.*, 2008), we intended to silence nta-miR399s by expressing the Arabidopsis *IPS1* gene in tobacco under the control of a CaMV (cauliflower mosaic virus) 35S promoter (Fig. S2a,b). Two transgenic lines were used, which were named oeIPS1-1 and oeIPS1-2. In the wild-type (WT) tobacco, −P treatment repressed the transcript levels of *PHO2-1* and *PHO2-2*, whereas in the oeIPS1-1 and oeIPS1-2 plants, −P treatment had little effect on the transcript levels of *PHO2-1* and *PHO2-2* (Fig. S2c–f). Importantly, compared with the WT plants, the oeIPS1-1 and oeIPS1-2 plants exhibited much lower mycorrhizal colonization efficiencies and decreased Pi contents in leaves and roots (Fig. S3). Thus, heterologous expression of Arabidopsis *IPS1* in tobacco inhibited the activity of nta-miR399s, leading to attenuated response of tobacco to Pi deficiency. Given that the two lines of oeIPS1 showed similar *PHO2* expression levels, colonization efficiencies, and Pi contents (Figs S2, S3) and large numbers of plants were needed to create dodder-connected tobacco clusters, we used the oeIPS1-1 line for the subsequent experiments.

To determine whether nta-miR399s are involved in dodder-mediated interplant Pi signaling, we created WT/oeIPS1 tobacco (SD)-dodder-WT tobacco (SR) clusters, and the AMF colonization efficiencies of the SR plants were quantified (Fig. 2a). Consistent with previous results (Fig. 1), in the WT tobacco-dodder-WT tobacco clusters, the AMF colonization efficiency of the SR plants increased when the SD plants were treated with −P (Fig. 2b). Importantly, in the oeIPS1 tobacco-dodder-WT tobacco clusters, the AMF colonization levels of the SR plants were similarly high, regardless of whether oeIPS1 tobacco plants were under the +P or −P conditions, reaching those of SR plants of WT tobacco-dodder-WT tobacco clusters under the −P conditions (Fig. 2b). Quantitative reverse transcription polymerase chain reaction analysis ruled out the possibility that *IPS1* transcripts can move from the oeIPS1 SD plants to dodder or SR plants (Fig. S4). Thus, nta-miR399s function as suppressors of the interplant systemic Pi signals: when *IPS1* was expressed in the SD tobacco to inhibit the activity of nta-miR399s, the systemic Pi signals were activated and transferred to the SR plants through dodder connections, resulting in increased AMF colonization.

CCD8 (carotenoid cleavage dioxygenase 8) is a key enzyme in the biosynthesis of SLs. Previously, tobacco *CCD8* genes were identified and the *ccd8* mutants exhibited typical SLs-deficient phenotypes (Gao *et al.*, 2018). Similarly, we knocked out the *CCD8* genes in tobacco using the CRISPR/Cas9 technology. As expected, the *ccd8* mutants (*ccd8*-1 and *ccd8*-2) all exhibited a phenotype of branching (Fig. S5a,b). *CCD8* was strongly upregulated by −Pi treatment in the WT plants, but not in the two *ccd8* lines (Fig. S5c). In Arabidopsis, the synthetic strigolactone analogue GR24 induces the expression of *BRC1*, thereby inhibiting the formation of plant branches (Wang *et al.*, 2020). We found that the levels of homologous gene *BRC1* in tobacco were upregulated by −P treatment in WT leaves but were always lower in the *ccd8* mutants (Fig. S5d). This is consistent with the over-branching phenotype of *ccd8* lines (Fig. S5b). These data well support that the identified tobacco *CCD8* genes are the bona fide *CCD8* genes of SLs biosynthesis. Colonization efficiencies in the two lines of *ccd8* mutants were significantly lower than those of WT plants (Fig. S6a), and the Pi contents in leaves and roots were also decreased (Fig. S6b,c), suggesting that SLs affect tobacco and AMF symbiosis and Pi homeostasis. Since *ccd8*-1 and *ccd8*-2 have similar phenotypes (Figs S5, S6), we only use *ccd8*-1 in the subsequent experiments.

To study whether SLs are involved in dodder-mediated systemic Pi signaling to regulate colonization of AMF, WT or *ccd8* plants were used as the SD plants to bridge connect with WT SR plants by dodders (Fig. 2c). Again, we detected increased AMF colonization efficiencies in the SR plants when the WT SD plants were treated with −P (Fig. 2d). However, when the *ccd8* mutants

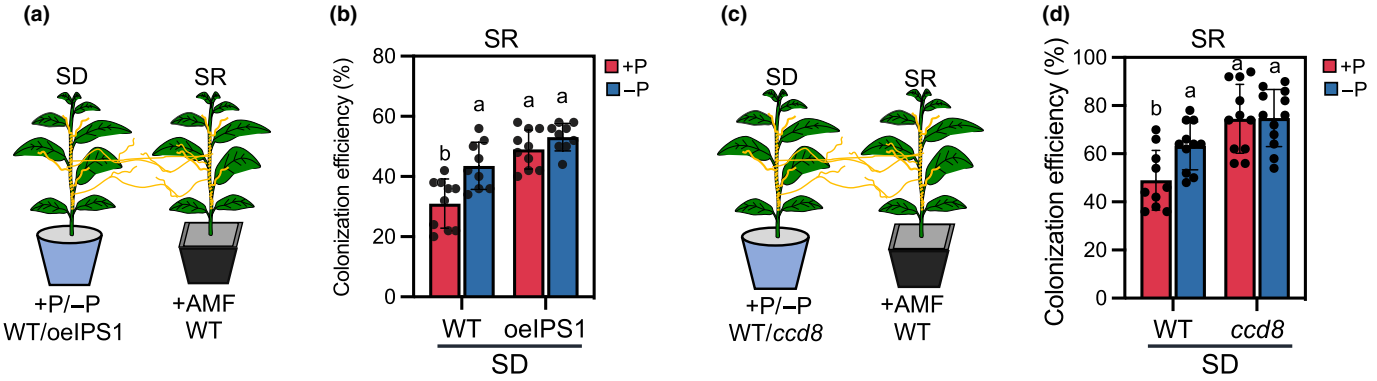

Fig. 2 Functions of microRNA399 (miR399) and strigolactone (SL) pathway of systemic signals donor plants in regulating interplant systemic phosphate signals-induced arbuscular mycorrhizal fungi (AMF) colonization in systemic signals receiver plants. (a, b) In wild-type (WT) tobacco-dodder-WT tobacco and oeIPS1 tobacco-dodder-WT tobacco plant clusters (a), the systemic signals donor (SD) plants were treated with phosphate (+P) or no phosphate (−P) conditions, and the systemic signals receiver (SR) plants were inoculated with AMF. After 18 d, AMF colonization efficiencies in the SR plants were measured (b). (c, d) In WT tobacco-dodder-WT tobacco and *ccd8* tobacco-dodder-WT tobacco plant clusters (c), the SD plants were treated with +P or −P conditions, and the SR plants were inoculated with AMF. After 18 d, AMF colonization efficiencies in the SR plants were measured (d). +P: 1 mM KH_2PO_4, −P: 0 mM KH_2PO_4. Data are mean ± standard deviation; n = 8–11. The experiment was repeated three times with similar results. Different letters indicate significant differences (one-way ANOVA by Tukey's multiple comparisons test; $P < 0.05$).

were the SD plants, the AMF colonization efficiencies in the SR plants increased to high levels, regardless of whether the SD plants were treated with −P or +P (Fig. 2d). Thus, similar to miR399s, SLs participate in dodder-mediated systemic Pi signaling as suppressors.

Next, we analyzed whether −P treatment on the SD plants or changes of colonization rates of AMF in the SR plants could alter the P contents of these plants. Our analyses indicated that 18 d after +P or −P treatment on the WT or oeIPS1 SD plants, there were no differences among the P concentrations of all SR plants, and the fresh and dry weights of SD, dodder, and SR plants from different groups of plant clusters were similar as well (Fig. S7a–e). Again, 18 d after +P or −P treatment on the WT or *ccd8* SD plants, the fresh and dry weights of dodders, SD, and SR plants from different plant clusters were very similar (Fig. S7f,g). Thus, these data support that no or very little amount of Pi could be transferred between host plants through dodder, and systemic Pi signals, but not changes of P status, enhanced AMF symbiosis efficiency in SR plants.

Strigolactone pathway inhibits the accumulation of nta-miR399s in systemic signal donor plants

Given that our genetic analyses indicated that silencing nta-miR399s or knocking out *CCD8* in the SD tobacco resulted in a similar AMF colonization phenotype in the SR tobacco, we speculated that SLs may regulate the level of nta-miR399s in the SD plants. To this end, we quantified the relative expression levels of nta-miR399s in the WT/*ccd8* (SD) tobacco-dodder-WT (SR) tobacco plant clusters (Fig. 3a). −P treatment highly induced the levels of nta-miR399s (20-fold) in the WT SD plants, and importantly, even much greater levels of nta-miR399s were detected in the *ccd8* SD plants (Fig. 3b), indicating that the SL pathway negatively regulates Pi deficiency-induced accumulation of nta-miR399s. We thus inferred that in the SD plants, the SL pathway inhibits the accumulation of nta-miR399s, and nta-miR399s negatively regulate Pi deficiency-induced systemic signals between dodder-connected different host plants.

The levels of nta-miR399s in the SR plants were much lower than SD plants (Fig. 3b). After the SR plants received the −P-induced interplant systemic signals, the levels of nta-miR399s increased only about twofold (Fig. 3b), while when *ccd8* was the SD plants, the nta-miR399s levels of the SR plants were similar to those of the SR plants in the WT tobacco-dodder-WT tobacco clusters after −P treatment (Fig. 3b). Notably, the levels of nta-miR399s in these SR plants of the WT tobacco-dodder-WT tobacco and *ccd8* tobacco-dodder-WT tobacco plant clusters were consistent with the efficiency of AMF colonization (Fig. 2d).

miR399 and strigolactone pathway-controlled systemic Pi signaling regulates transcriptomes of systemic signals receiver plants

When SD plants were oeIPS1 or *ccd8* plants, the SR plants exhibited increased AMF colonization rates, regardless of whether SD plants were treated with −P or +P (Fig. 2). Thus, it is possible that SL- and miR399-regulated interplant systemic signals from SD plants could converge on controlling certain common genes in the SR plants which function in regulating AMF colonization.

In WT/oeIPS1/*ccd8* (SD) tobacco-dodder-WT (SR) tobacco clusters, the SD plants were treated with −P or +P, and the SR plants were immediately inoculated with AMF (Fig. 2a,c). After 18 d, the roots of SR plants were harvested for transcriptome (RNA-Seq) analysis. The differentially expressed genes (DEGs) between the SR plants in the WT/oeIPS1 tobacco (SD)-dodder-WT tobacco (SR) clusters were identified (named oeIPS1 vs WT) (Fig. 4a; Table S3). Similarly, the DEGs were obtained by comparing the SR plants in the WT/*ccd8* tobacco (SD)-dodder-WT tobacco (SR) clusters (named *ccd8* vs WT) (Fig. 4b;

New Phytologist

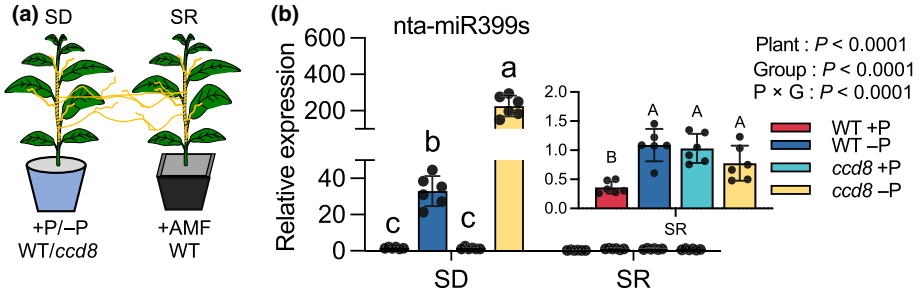

Fig. 3 Relative expression levels of microRNA399s (miR399s) in tobacco host plants of the dodder-connected plant clusters. (a) Schematic of wild-type (WT) tobacco (*N. tabacum*)-*dodder* (*C. campestris*)-*WT* tobacco and *ccd8* tobacco-dodder-WT tobacco clusters. The systemic signals donor (SD) plants were treated with phosphate (+P) or no phosphate (−P) conditions, and the systemic signals receiver (SR) plants were inoculated with arbuscular mycorrhizal fungi (AMF). After 18 d, leaves of SD and SR plants were harvested. (b) Relative expression levels of nta-miR399s in SD and SR plants. Inset: zoom-in view of data from SR plants. +P: 1 mM KH_2PO_4, −P: 0 mM KH_2PO_4. Data are mean ± standard deviation; $n = 6$. Two-way ANOVA analysis followed by Tukey test were performed for comparison of SD data with SR data (P indicate significance level). One-way ANOVA analysis followed by Tukey test were performed for different samples in SD and SR data. Different letters indicate significant differences (one-way ANOVA by Tukey's multiple comparisons test; $P < 0.05$, small letter for SD, capital letter for SR).

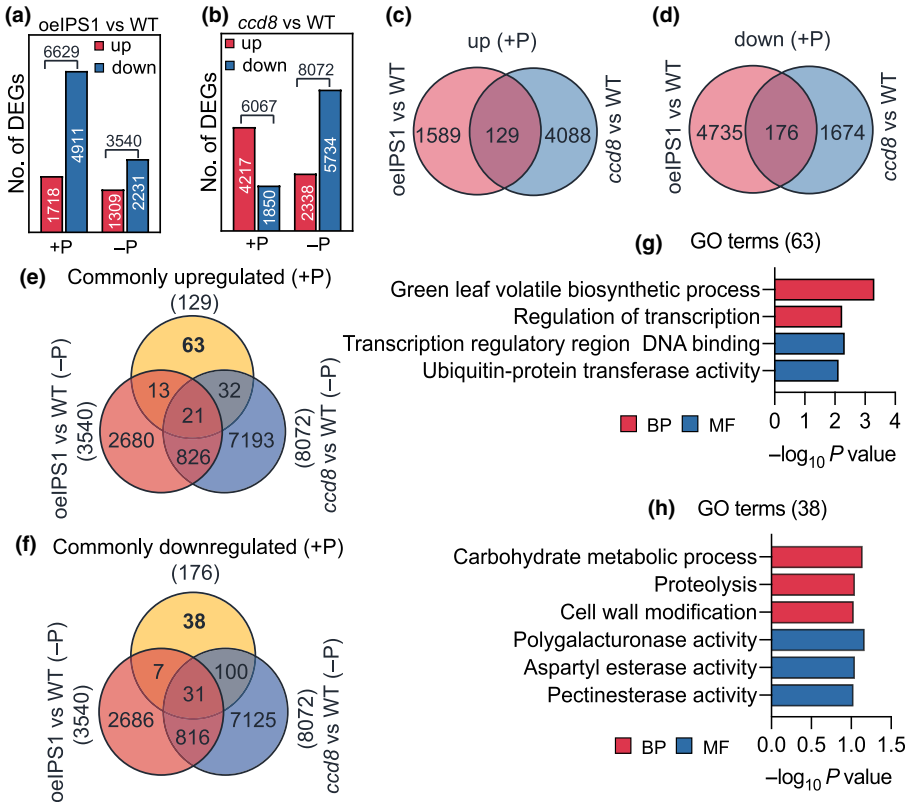

Fig. 4 Role of microRNA399 (miR399) and strigolactone (SL) pathway in systemic signals donor plants in regulating transcriptomes of systemic signals receiver plants' roots. In wild-type (WT)/oeIPS1/*ccd8* tobacco (*N. tabacum*) (systemic signals donor, SD)-dodder (*C. campestris*)-*WT* tobacco (systemic signals receiver, SR) plant clusters, the SD plants were treated with phosphate (+P) or no phosphate (−P) conditions, and the SR plants were inoculated with arbuscular mycorrhizal fungi (AMF). After 18 d, the roots of SR plants were harvested for transcriptome analysis. (a, b) Numbers of up- and downregulated differentially expressed genes (DEGs) identified between root transcriptomes of SR plants connected with oeIPS1 and WT tobacco as SD plants, respectively (oeIPS1 vs WT) (a), and between root transcriptomes of SR plants connected with *ccd8* and WT tobacco as SD plants, respectively (*ccd8* vs WT) (b). (c, d) Venn diagram analysis of the up- (c) and downregulated (d) DEGs from oeIPS1 vs WT and DEGs from *ccd8* vs WT under +P conditions. (e) Venn diagram analysis of the 129 commonly upregulated genes identified in (c) and the DEGs obtained from oeIPS1 vs WT and *ccd8* vs WT under −P conditions. (f) Venn diagram analysis of the 176 commonly downregulated genes identified in (d) and the DEGs obtained from oeIPS1 vs WT and *ccd8* vs WT under −P conditions. (g) Enriched gene ontology (GO) terms from the 63 specifically upregulated genes identified in (e). (h) Enriched GO terms from the 38 specifically downregulated genes identified in (f). WT, oeIPS1, and *ccd8* indicate the genotypes of SD plants. BP, biological process, MF, molecular function. +P: 1 mM KH_2PO_4, −P: 0 mM KH_2PO_4. All data can be found in Supporting Information Tables S3–S7.

Table S3). These two sets of DEGs were used for further Venn diagram analysis to identify the commonly regulated genes, which may be located downstream of both SLs- and miR399s-regulated interplant systemic signals in the SR plants and function in AMF colonization.

We found that 129 up- and 176 downregulated DEGs were common between the DEGs of oeIPS1 vs WT and *ccd8* vs WT under +P condition (Fig. 4c,d; Table S4). Given that under −P conditions, all the SR plants in the WT/oeIPS1-dodder-WT tobacco clusters and WT/*ccd8* tobacco-dodder-WT tobacco clusters showed similar higher AMF colonization than did the WT tobacco-dodder -WT tobacco clusters under +P conditions (Fig. 2), it is possible that the key genes involved in regulation of AMF colonization in the SR plants have similar expression levels between the SR plants connected with WT SD plants and the SR plants connected with oeIPS1 or *ccd8* plants. Thus, we screened for the genes, which were commonly up- or downregulated DEGs under +P condition but were not DEGs under −P condition. In this manner, 63 up- and 38 downregulated genes were found to be the candidate genes that are possibly involved in AMF colonization (Fig. 4e,f; Table S4). These 63 upregulated genes included an auxin-responsive gene, a high-affinity nitrate transporter, and five transcription factors (Fig. S8; Table S4). Gene ontology (GO) analysis indicated enrichment of the biological process and molecular function terms related to transcription (Fig. 4g; Table S5), suggesting that both SL- and miR399-regulated interplant systemic signaling increased AMF colonization by enhancing transcriptional regulation in the SR plants. The 38 downregulated genes included an ethylene-responsive transcription factor, a nonspecific lipid-transfer protein, and a probable calcium-binding protein (Fig. S9; Table S4). The GO terms 'carbohydrate metabolic process' of biological processes and 'polygalacturonase activity, aspartyl esterase activity, and pectinesterase activity' of molecular function were enriched form the 38 downregulated genes (Fig. 4h; Table S5), implying that SL- and miR399-regulated interplant systemic signaling may regulate some enzymes' activity leading to the increased AMF colonization efficiency in SR plants.

Notably, under either −P or +P conditions, many specific DEGs were detected between the SR plants in the WT/oeIPS1 tobacco (SD)-dodder-WT tobacco (SR) clusters and between the SR plants in the WT/*ccd8* tobacco (SD)-dodder-WT tobacco (SR) clusters (Fig. S10a; Table S4). GO analysis indicated enrichment of different terms of biological processes from these specific DEGs. 'Phosphate ion transport' was among the top 10 enriched terms from the specifically upregulated DEGs in the SR plants of WT/oeIPS1 tobacco-dodder-WT tobacco clusters (Fig. S10b; Table S6), while the specifically upregulated DEGs in the SR plants of WT/*ccd8* tobacco-dodder-WT tobacco clusters showed enrichment of 'coumarin biosynthetic process' among the top 10 terms (Fig. S10c; Table S7). Notably, coumarin is involved in plant–microbial interactions, including AMF (Stassen *et al.*, 2021; Mohammed *et al.*, 2022). These data suggest that in addition to their common function in regulating AMF colonization, SL and miR399 pathway in the SD plants have different functions in regulating systemic responses in the SR plants.

miR399- and strigolactone-regulated interplant Pi signals shape the rhizosphere bacterial assembly in systemic signals receiver plants

In addition to the mycorrhizal pathway, AMF recruit hyphosphere microbes, and this process is also crucial for acquisition of soil organic P (Wang *et al.*, 2022). Since the miR399 and SL signaling of SD plants control AMF symbiosis efficiency of the SR plants, we hypothesized that these signaling pathways may also affect the rhizosphere bacterial communities of SR plants.

Thus, we established the WT/oeIPS1 tobacco (SD)-dodder-WT tobacco (SR) clusters, and the rhizosphere soil of the SR plants was collected for further analyses. In the WT tobacco-dodder-WT tobacco clusters, the acid phosphatase (ACP) activity of SR plants' rhizosphere soil reduced when the SD plants were treated with −P, and so was the ACP activity of the SR plants' rhizosphere soil in the oeIPS1 tobacco-dodder-WT tobacco clusters under both +P or −P condition (Fig. S11a). However, the alkaline phosphatase (ALP) activity was similar across the four groups of SR rhizosphere soil in WT/oeIPS1 tobacco-dodder-WT tobacco clusters under +P and −P conditions (Fig. S11b). Then, we carry out 16S rRNA profiling for the SR rhizosphere soil (Fig. 5a). The USEARCH (Edgar, 2010) software was used to cluster reads at a similarity level of 97.0% to obtain OTUs (Operational Taxonomic Units) (Table S8). First, we analyzed the alpha diversity of the rhizosphere bacteria in the SR plants. The Shannon index, Simpson index, and Richness showed no significant differences between the SR plants of WT tobacco-dodder-WT tobacco and oeIPS1 tobacco-dodder-WT tobacco under both +P and −P conditions (Fig. 5b–d; Table S9), suggesting that neither −P treatment nor miR399 signaling affects the diversity of rhizosphere bacterial communities of SR plants. After removing OTUs in low abundance (sequences numbers < 10 in each group) (Table S10), we used Venn diagram to analyze the rhizosphere microbes of different SR plants under both −P and +P conditions and found 1238 core OTUs (77.3% of all OTUs) (Fig. 5e; Table S11). Importantly, −P treatment on the SD plants greatly changed the relative abundance of rhizosphere communities of the SR plants at the phylum level (Fig. 5f; Table S12). Functional profiles showed that 13 significantly different KEGG metabolic pathways were enriched from the rhizosphere bacterial communities of SR plants of WT/oeIPS1 tobacco-dodder-WT tobacco clusters, most of them were highest in the rhizosphere communities of SR plants in WT tobacco-dodder-WT tobacco clusters under −P condition (Fig. S12; Table S13).

In the WT/*ccd8* tobacco (SD)-dodder-WT tobacco (SR) clusters (Fig. 5g), the ACP activity in the four groups SR rhizosphere soil were similar (Fig. S11c), but the ALP activity in the SR rhizosphere soil was decreased when *ccd8* mutants were the SD plants compared with that in the rhizosphere soil of SR plants from the other three groups (Fig. S11d). 16S rRNA profiling did not show differences in the diversity of rhizosphere bacteria in the SR plants (Fig. 5h–j; Table S9). After removing the OTUs with low abundance (Table S10), Venn diagram analysis indicated that 1365 OTUs (83.2% of all the OTUs) co-existed in the

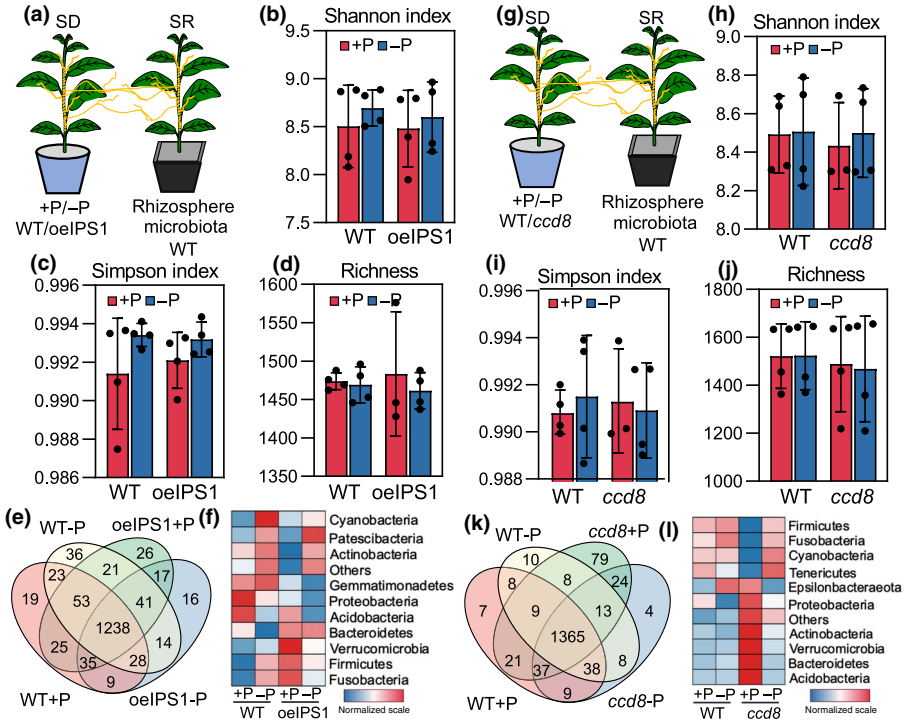

Fig. 5 Regulatory functions of microRNA399 (miR399) and strigolactone (SL) pathway in the systemic signals donor plants on the rhizosphere bacterial communities of systemic signals receiver plants. In wild-type (WT) tobacco (*N. tabacum*)-*dodder* (*C. campestris*)-*WT* tobacco and oeIPS1 tobacco-dodder-WT tobacco plant clusters (a), the systemic signals donor (SD) plants were treated with phosphate (+P) or no phosphate (−P) conditions. After 18 d, rhizosphere bacterial communities of the systemic signals receiver (SR) plants were analyzed for the alpha diversity (Shannon index (b), Simpson index (c), Richness (d)), the common and unique Operational Taxonomic Units (OTUs) (e), and the relative abundance of bacterial communities at the phylum level (f). Same experiment was done for the WT tobacco-dodder-WT tobacco and *ccd8* tobacco-dodder-WT tobacco plant clusters (g), and the rhizosphere bacterial communities of the SR plants were analyzed for the alpha diversity (h–j), the common and unique OTUs (k), and the relative abundance of bacterial communities at the phylum level (l). WT, oeIPS1, and *ccd8* indicate the genotypes of SD plants. +P: 1 mM KH_2PO_4, −P: 0 mM KH_2PO_4. Data are mean ± standard deviation; n = 3–4. All the data can be obtained in Supporting Information Tables S8–S12.

rhizosphere of the SR plants of WT/*ccd8* tobacco (SD)-dodder-WT tobacco (SR) clusters, regardless of +P or −P nutrient conditions (Fig. 5k; Table S11). Again, at the phylum level, the relative abundance of rhizosphere bacterial communities of the SR plants in the *ccd8* tobacco-dodder-WT tobacco system was very different from that in the WT tobacco-dodder-WT tobacco system (Fig. 5l; Table S12). The top 20 most significantly different KEGG pathways enriched from the rhizosphere bacterial communities of SR plants of WT/*ccd8* tobacco-dodder-WT tobacco clusters included the term 'Phosphonate and phosphinate metabolism' (Fig. S13; Table S13).

From these data, we inferred that miR399 and SL pathway-mediated Pi systemic signaling plays important roles in shaping the rhizosphere bacterial communities of the SR plants, and likely affects the interactions between the SR plants and rhizosphere microbial communities.

miR399 and strigolactone pathway in systemic signals receiver plants affect AMF colonization

Previous research has revealed that miR399s and SLs function in plant association with AMF (Müller & Harrison, 2019). It is plausible that these two pathways may also be involved in the process of AMF colonization when plants receive Pi deficiency-induced systemic signals from the neighboring plants through dodder connections. To test this hypothesis, WT tobacco (SD)-dodder-WT/oeIPS1/*ccd8* tobacco (SR) clusters were set up, in which WT tobacco served as the SD plants and were treated with +P or −P, and the SR plants were inoculated with AMF (Fig. 6a).

In the WT tobacco-dodder-WT tobacco system, we found that −P treatment on the SD plants increased the AMF symbiosis efficiency in the SR plants (Fig. 6b,c). Importantly, in the WT tobacco (SD)-dodder-oeIPS1 tobacco (SR) and WT tobacco (SD)-dodder-*ccd8* tobacco (SR) clusters, regardless of whether the WT SD plants were treated with −P or +P, the oeIPS1 and *ccd8* SR plants exhibited increased AMF symbiosis efficiency to similar levels as those of the SR plants in the −P-treated WT tobacco-dodder-WT tobacco clusters (Fig. 6b,c). Therefore, miR399 and SL pathway both suppress AMF symbiosis in the SR plants of such a host-dodder-host system.

Pi deficiency promotes interplant movement miR399s between dodder and tobacco

Long-distance movement of miR399s from shoot to root has been well documented in individual plants (Pant *et al.*, 2008; Chiang *et al.*, 2023). Thus, we hypothesized that interplant movement of miR399s may also occurs in such dodder-connect

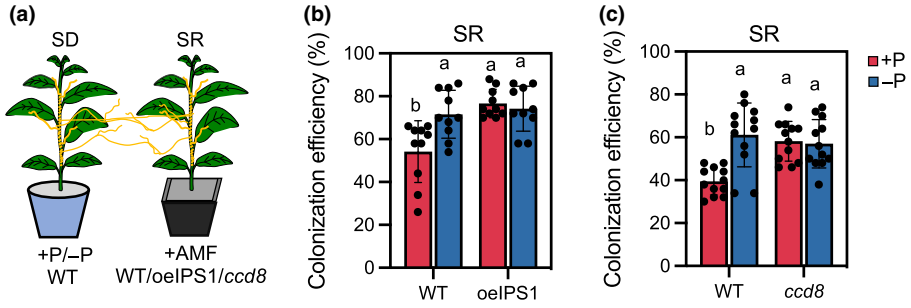

Fig. 6 Functions of microRNA399 (miR399) and strigolactone (SL) pathway of systemic signals receiver (SR) plants in regulating interplant systemic phosphate signals-induced arbuscular mycorrhizal fungi (AMF) colonization. In wild-type (WT) tobacco (*N. tabacum*)-*dodder* (*C. campestris*)-*WT* tobacco, WT tobacco-dodder-oeIPS1 tobacco, and WT tobacco-dodder-*ccd8* tobacco plant clusters (a), the systemic signals donor (SD) plants were treated with phosphate (+P) or no phosphate (−P) conditions, and the SR plants were inoculated with AMF. After 18 d, AMF colonization efficiencies in the SR plants were measured (b, c). +P: 1 mM KH_2PO_4, −P: 0 mM KH_2PO_4. Data are mean ± standard deviation; n = 10–12. The experiment was repeated three times with similar results. Different letters indicate significant differences (one-way ANOVA with Tukey's multiple comparisons test; $P < 0.05$).

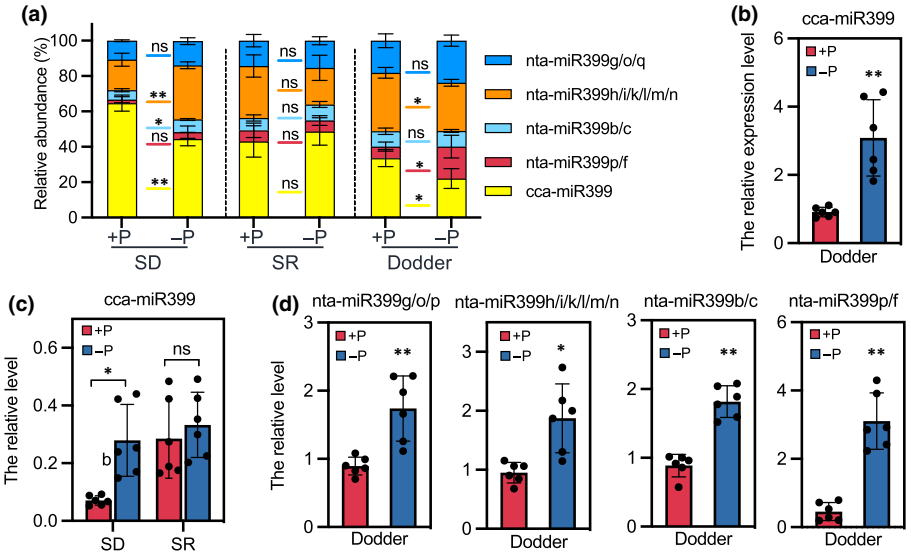

Fig. 7 Interplant movement of microRNA399s (miR399s) between dodder and tobacco in tobacco-dodder-tobacco plant clusters. In wild-type (WT) tobacco (*N. tabacum*)-*dodder* (*C. campestris*)-*WT* tobacco plant clusters, the systemic signal donor (SD) plants were treated with phosphate (+P) or no phosphate (−P) conditions, and the systemic signals receiver (SR) plants were inoculated with arbuscular mycorrhizal fungi (AMF). After 18 d, leaves of SD and SR plants and dodder were harvested for stem-loop real-time polymerase chain reaction amplification of tobacco nta-miR399s and dodder cca-miR399. (a) Relative abundance of four nta-miR399s and one cca-miR399 in SD, SR, and dodder plants. Asterisks above the color horizontal lines indicate significant differences between +P and −P treatment for the indicated miR399. (b) Relative expression levels of cca-miR399 in dodder. (c) Relative levels of cca-miR399 in SD and SR plants. (d) Relative levels of nta-miR399s in dodder. +P: 1 mM KH_2PO_4, −P: 0 mM KH_2PO_4. Data are means ± standard deviation; n = 3–4 for (a), n = 6 for (b–d). Asterisks indicate significant differences (Student's t-test, $^*P < 0.05$, $^{**}P < 0.01$). ns, not significant.

plant clusters. We constructed WT tobacco (SD)-dodder-WT tobacco (SR) plant clusters, and the SD plants were treated with +P and −P conditions. nta-miR399s of tobacco (Frazier *et al.*, 2010) and cca-miR399 of dodder (Zangishei *et al.*, 2022) were specifically amplified from both host plants and dodder using stem-loop reverse transcription polymerase chain reaction, and the PCR products were used for Next-Generation sequencing. Four tobacco nta-miR399s sequences and one dodder cca-miR399 sequence were amplified and the sequencing data clearly indicated that tobacco nta-miR399s could move to dodder and dodder cca-miR399 could move to SD and SR tobacco hosts (Fig. 7a; Table S14). The relative abundance of total nta-miR399h/i/k/l/m/n and nta-miR399b/c detected in the SD plants was greater under −P conditions than under +P conditions (Fig. 7a), and the relative abundance of cca-miR399 was lower in the −P-treated SD plants than in the +P-treated SD plants (Fig. 7a). All the miR399s did not change their relative abundance in SR plants under +P and −P conditions. Specifically, we analyzed the levels of cca-miR399 in dodder and in SD and SR tobacco. cca-miR399 levels were induced about two times when SD plants were treated with −P (Fig. 7b); increased levels of cca-miR399 were also detected in the −P-treated SD

tobacco plants, compared with the +P-treated SD plants, while the cca-miR399 levels in the SR plants were similar to those in the −P-treated SD tobacco plants under both +P and −P conditions (Fig. 7c). Quantification of tobacco nta-miR399s in dodder indicated that more nta-miR399s moved from tobacco hosts to dodder under −P conditions than under +P conditions, and this is consistent with the highly increased levels of miR399s in the −P-treated SD plants (Fig. 3b). These results suggest that miR399s can travel between dodder and hosts, and Pi deficiency enhances the movement of miR399s between SD and dodder, but the movement from dodder to SR plants is not affected by the SD plants' P status.

Discussion

A dodder parasite can simultaneously connect two or multiple adjacent plants, forming a dodder-connected plant cluster (Hettenhausen *et al.*, 2017). AMF play important roles in providing plants with nitrogen (N) and Pi nutrients. In this study, we show that dodder can transmit Pi deficiency-induced systemic signals to Pi-replete plants and activate physiological changes that allow increased AMF colonization and changes of rhizosphere bacterial communities. Importantly, our genetic analyses indicated that the miR399 and SL pathways negatively control interplant systemic Pi signals, and these two pathways also suppresses AMF colonization in the dodder-connected systemic SR plants.

Dodders are holoparasitic plants. All the water and nutrients required for their growth and development are extracted from the host plants. It was expected that due to nutrient deprivation by dodder, the tobacco hosts may suffer from N and Pi nutrient deficiency and thus increase symbiosis with AMF. However, we found that under both +P and −P conditions, dodder parasitism decreased the efficiency of AMF colonization in tobacco roots, compared to the efficiency of AMF colonization in the roots of nonparasitized tobacco plants (Fig. S1). It is possible that dodder parasitism greatly restricts nutrient supply of the host to AMF (e.g. carbohydrates and lipids), thereby reducing AMF colonization, and/or dodder parasitism alters certain signaling pathways of the host plant, which are involved in plant–AMF interactions, resulting in decrease of AMF colonization. Similarly, Yuan & Li (2022) reported that dodder parasitization decreased AMF colonization rate in *Bidens pilosa*.

Our genetic analysis indicated that the miR399 and SL pathways are involved in dodder-mediated systemic Pi signaling between host plants and these two pathways affect AMF colonization in the SR plant roots (Fig. 2). Thus, both the SL and miR399 pathways suppress the interplant Pi signals produced by the SD plants, which promote AMF colonization in the SR plants. Importantly, at the transcriptional level, the SL pathway is likely located upstream of miR399s to regulate the interplant Pi signaling (Fig. 3). In individual plants, many molecules, such as Pi, miRNAs, phytohormones, and sugars, can act as signals in activating systemic Pi response (Yang *et al.*, 2024). However, the exact nature of the mobile signals remains elusive (Chiou & Lin, 2011; Lambers, 2022). Given the special parasitic physiology of dodder, the vascular connections of dodder with hosts might be different from the within-plant vascular systems, and this may influence the signal transfer between dodder and hosts: dodder may filter and even modify the interplant systemic signals to manipulate the physiology of host plants for the advantages of dodder. Future research should focus on identifying the nature of the interplant systemic Pi signals and the precise mechanisms of interplant systemic Pi signaling in dodder-connected plant clusters.

It has been well demonstrated that miR399s are mobile Pi signals from shoot to root (Lin *et al.*, 2008; Chiang *et al.*, 2023). Consistently, our analysis indicated that miR399s can move from hosts to dodder and from dodder to hosts, and Pi deficiency treatment on the SD plants enhanced the movement of miR399s between SD and dodder, but the movement of cca-miR399 from dodder to SR was not affected by the P status of SD plants (Fig. 7; Table S14). Although we could not determine whether nta-miR399s can travel between the SD and SR plants, it seems that nta-miR399s from the SD plants can hardly move into SR plants through dodder: in the *ccd8* tobacco-dodder-WT tobacco clusters, even though after −P treatment, the *ccd8* SD plants contained highly elevated levels of nta-miR399s, the levels of nta-miR399s in the SR plants only very slightly changed (Fig. 3b). Therefore, nta-miR399s are unlikely to be the systemic Pi signals from SD to SR plants. Bioinformatic analysis predicted that the dodder cca-miR399 could target the tobacco *PHO2* sequence (Zangishei *et al.*, 2022), suggesting that dodder cca-miR399 may play a role in host Pi signaling. The physiological role of such interplant transfer of miR399s between dodder and SD and between dodder and SR plants deserves to be studied.

Our genetic evidence also revealed that in the SR plants, the SL and miR399 pathways both play negative roles in modulating AMF colonization (Fig. 6). Furthermore, both pathways likely function downstream of the interplant mobile Pi signals to control AMF colonization efficiency, as it was found that the oeIPS1 and *ccd8* SR plants all exhibited increased AMF colonization under both +P and −P conditions (Fig. 6). The SL pathway negatively controls the levels of nta-miR399s in SD plants under −P conditions (Fig. 3b). Whether the SL signaling pathway transcriptionally regulates nta-miR399s in the SR plants and thus modulates AMF colonization worth further investigation. Notably, in individual plants SLs are often positively associated with AMF symbiosis (Choi *et al.*, 2020), as SLs are secreted by root to rhizosphere where they activate AMF spore germination and hyphae branching (Kretzschmar *et al.*, 2012). However, the biosynthesis mutants of SLs can still be partially or fully colonized by AMF and form normal arbuscular structures (Gomez-Roldan *et al.*, 2008), indicating that in addition to SLs, there are other signaling molecules that mediate the perception of the host plant with AMF, such as flavonoids (Bécard *et al.*, 1992), N-acetylglucosamine (Nadal *et al.*, 2017), 2-hydroxid fatty acids (Nagahashi & Douds, 2011). The obvious discrepancy between the SL pathway's functions in the SR plants and individual plants led us to hypothesize that in the SR plants, certain unknown signaling is suppressed by SL (and miR399), and this unknown signaling pathway also plays an important role in the symbiosis between tobacco and AMF.

The total P concentration in SR plants of WT/oeIPS1 tobacco (SD)-dodder-WT tobacco (SR) plant clusters, and the fresh and dry weights of all plants in dodder-connected plant clusters, under +P or −P conditions, regardless of the genotypes of SD plants, did not detect any obvious changes (Fig. S7a–g), indicating that after −P treatment, the increased AMF colonization in the SR plants was due to certain systemic signals from the SD plants, but not changes in P levels in SR plants. We speculated that there were two possible reasons for these results: (1) Dodders are parasites, which are specialized in taking up nutrients and water from hosts; and thus these parasites do not allow transfer of nutrients to host plants or these parasites transfer very small amount of nutrients between hosts, which have no obvious effects on host plants. Similarly, in our previous study, it was found that dodder could transfer bidirectional systemic N signals between host plants; however, N transfer between host plants was not detected in the ^{15}N labeling experiments (Zhang *et al.*, 2021); (2) the SR tobacco plants were watered with MHS (containing 1 mM KH_2PO_4), and as a result, the SR tobacco roots could have directly absorbed Pi and did not much relied on the mycorrhiza. This could be the reason why the increased AMF symbiosis rates did not improve the total P contents in the SR plants.

Obviously, in addition to AMF, the SL- and miR399-regulated interplant mobile signals also modulate SR plants' rhizosphere microbial communities (Fig. 5). However, unlike their similar functions in controlling AMF colonization, these two pathways shape different relative abundance of the bacteria, confirming that SL- and miR399-regulated interplant mobile signals are likely somewhat different. Our transcriptome analysis revealed that the transcriptomes of the SR tobacco plants in the WT/oeIPS1/*ccd8* tobacco (SD)-dodder-WT tobacco (SR) clusters are largely different (Fig. S10). We speculate that these mobile signals from oeIPS1 tobacco and *ccd8* tobacco differentially affect the physiology of SR plants, resulting in changes of release of signaling molecules and/or nutrients from the roots of SR plants and thus affecting the assembly of bacterial microbes.

Taken together, using the host plant-dodder-host plant clusters, we demonstrated that dodder transmits interplant systemic Pi signals from Pi-stressed host plants to other Pi-replete hosts and that these signals activate large physiological changes in the SR plant, resulting in altered root transcriptome, increased AMF colonization, and changes of rhizosphere bacterial communities. Importantly, the SL and miR399 pathways play dual roles: they not only negatively control the production and/or transport of the systemic Pi signals in the Pi-starved SD plants, but also suppress AMF colonization in the Pi-replete SR plants. These findings expand our understanding of roles of dodder from mediating plant–plant interactions to orchestrating plant–rhizosphere microbe interactions and highlight the importance of SLs and miR399s in systemic Pi signaling between plants and likely in individual plants. This study focused mainly on dodder-mediated interplant Pi signaling, future studies should address the ecological outcome of such interplant signaling using more ecologically oriented settings, including the cultivation of plants in large volume of soil and substantially longer coculture time with AMF.

Acknowledgements

This work was supported by National Natural Science Foundation of China (32100251 (JZ), 32270314 (GS)), the Key Project of Applied Basic Research Program of Yunnan Province (202201AS070056 (JW), 202301AS070064 (GS)), WRLJ Program of Ministry of Science and Technology of China (JW), Yunnan Revitalization Talent Support Program 'Yunling Scholar' Project of Yunnan Province (JW), the Special Research Assistant of Chinese Academy of Sciences (JZ), and Yunnan Revitalization Talent Support Program 'Young Talents' Project of Yunnan Province (XDYC-QNRC-2022-0301 (JZ), XDYC-QNRC-2022-0001 (GS)), Chinese Academy of Sciences (CAS) Light of West China Program (GS). We would like to express our gratitude to Drs. Wei Chang and Fei Li (Kunming Institute of Botany, CAS) for their invaluable technical support. We thank Dr Nianwu Tang (Guangxi Institute of Botany) for kindly providing *Rhizophagus irregularis*.

Competing interests

None declared.

Author contributions

JW, JZ and MZ designed the study. MZ, JZ, XZ, GS, ZF, WL, GC and SZ performed the experiments. MZ, ZS, JZ, YX and JW carried out data analyses. MZ, JZ and JW wrote and revised the manuscript. All the authors read and approved the final manuscript.

ORCID

Guoyan Cao https://orcid.org/0000-0002-3807-7762
Zerui Feng https://orcid.org/0000-0002-0034-8520
Wenxing Li https://orcid.org/0000-0001-5377-6687
Guojing Shen https://orcid.org/0000-0001-9655-9172
Zhongxiang Su https://orcid.org/0000-0002-0056-7635
Jianqiang Wu https://orcid.org/0000-0002-7726-6216
Yuxing Xu https://orcid.org/0000-0002-7801-8759
Jingxiong Zhang https://orcid.org/0000-0003-4490-6309
Shuhan Zhang https://orcid.org/0000-0002-3659-9049
Man Zhao https://orcid.org/0000-0003-0246-061X
Xijie Zheng https://orcid.org/0000-0003-1635-2433

Data availability

All data supporting the findings are contained in this manuscript. Transcriptome, rhizosphere bacterial community data, and miR399s sequencing data are, respectively, available from BIG BioProject (BioProject – CNCB-NGDC): PRJCA011150, PRJCA017889, and PRJCA023358. Additional supporting information may be found in Figs S1–S13; Methods S1; Tables S1–S14.

References

Alder A, Jamil M, Marzorati M, Bruno M, Vermathen M, Bigler P, Ghisla S, Bouwmeester H, Beyer P, Al-Babili S. 2012. The path from beta-carotene to carlactone, a strigolactone-like plant hormone. *Science* **335**: 1348–1351.

Aung K, Lin SI, Wu CC, Huang YT, Su CL, Chiou TJ. 2006. pho2, a phosphate overaccumulator, is caused by a nonsense mutation in a MicroRNA399 target gene. *Plant Physiology* **141**: 1000–1011.

Barbier F, Fichtner F, Beveridge C. 2023. The strigolactone pathway plays a crucial role in integrating metabolic and nutritional signals in plants. *Nature Plants* **9**: 1191–1200.

Bari R, Pant BD, Stitt M, Scheible WR. 2006. PHO2, microRNA399, and PHR1 define a phosphate-signaling pathway in plants. *Plant Physiology* **141**: 988–999.

Bécard G, Douds DD, Pfeffer PE. 1992. Extensive *in vitro* hyphal growth of vesicular-arbuscular mycorrhizal fungi in the presence of CO(2) and Flavonols. *Applied and Environmental Microbiology* **58**: 821–825.

Bennett AE, Groten K. 2022. The costs and benefits of plant-arbuscular mycorrhizal fungal interactions. *Annual Review of Plant Biology* **73**: 649–672.

Branscheid A, Sieh D, Pant BD, May P, Devers EA, Elkrog A, Schauser L, Scheible WR, Krajinski F. 2010. Expression pattern suggests a role of MiR399 in the regulation of the cellular response to local Pi increase during arbuscular mycorrhizal symbiosis. *Molecular Plant–Microbe Interactions* **23**: 915–926.

Chiang CP, Li JL, Chiou TJ. 2023. Dose-dependent long-distance movement of microRNA399 duplex regulates phosphate homeostasis in Arabidopsis. *New Phytologist* **240**: 802–814.

Chien PS, Chiang CP, Leong SJ, Chiou TJ. 2018. Sensing and signaling of phosphate starvation: from local to long distance. *Plant and Cell Physiology* **59**: 1714–1722.

Chiou TJ, Lin SI. 2011. Signaling network in sensing phosphate availability in plants. *Annual Review of Plant Biology* **62**: 185–206.

Choi J, Lee T, Cho J, Servante EK, Pucker B, Summers W, Bowden S, Rahimi M, An K, An G *et al.* 2020. The negative regulator SMAX1 controls mycorrhizal symbiosis and strigolactone biosynthesis in rice. *Nature Communications* **11**: 2114.

Das D, Paries M, Hobecker K, Gigl M, Dawid C, Lam HM, Zhang JH, Chen MX, Gutjahr C. 2022. PHOSPHATE STARVATION RESPONSE transcription factors enable arbuscular mycorrhiza symbiosis. *Nature Communications* **13**: 477.

Duan SL, Declerck S, Feng G, Zhang L. 2023. Hyphosphere interactions between *Rhizophagus irregularis* and *Rahnella aquatilis* promote carbon-phosphorus exchange at the peri-arbuscular space in *Medicago truncatula*. *Environmental Microbiology* **25**: 867–879.

Edgar RC. 2010. Search and clustering orders of magnitude faster than BLAST. *Bioinformatics* **26**: 2460–2461.

Franco-Zorrilla JM, Valli A, Todesco M, Mateos I, Puga MI, Rubio-Somoza I, Leyva A, Weigel D, García JA, Paz-Ares J. 2007. Target mimicry provides a new mechanism for regulation of microRNA activity. *Nature Genetics* **39**: 1033–1037.

Frazier TP, Xie FL, Freistaedter A, Burklew CE, Zhang BH. 2010. Identification and characterization of microRNAs and their target genes in tobacco (*Nicotiana tabacum*). *Planta* **232**: 1289–1308.

Gao J, Zhang T, Xu B, Jia L, Xiao B, Liu H, Liu L, Yan H, Xia Q. 2018. CRISPR/Cas9-mediated mutagenesis of carotenoid cleavage dioxygenase 8 (CCD8) in tobacco affects shoot and root architecture. *International Journal of Molecular Sciences* **19**: 1062.

Gomez-Roldan V, Fermas S, Brewer PB, Puech-Pages V, Dun EA, Pillot JP, Letisse F, Matusova R, Danoun S, Portais JC *et al.* 2008. Strigolactone inhibition of shoot branching. *Nature* **455**: 189–194.

Hettenhausen C, Li J, Zhuang HF, Sun HH, Xu YX, Qi JF, Zhang JX, Lei YT, Qin Y, Sun GL *et al.* 2017. Stem parasitic plant *Cuscuta australis* (dodder) transfers herbivory-induced signals among plants. *Proceedings of the National Academy of Sciences, USA* **114**: E6703–E6709.

Jiang YN, Wang WX, Xie QJ, Liu N, Liu LX, Wang DP, Zhang XW, Yang C, Chen XY, Tang DZ *et al.* 2017. Plants transfer lipids to sustain colonization by mutualistic mycorrhizal and parasitic fungi. *Science* **356**: 1172–1175.

Kim G, LeBlanc ML, Wafula EK, dePamphilis CW, Westwood JH. 2014. Genomic-scale exchange of mRNA between a parasitic plant and its hosts. *Science* **345**: 808–811.

Kretzschmar T, Kohlen W, Sasse J, Borghi L, Schlegel M, Bachelier JB, Reinhardt D, Bours R, Bouwmeester HJ, Martinoia E. 2012. A petunia ABC protein controls strigolactone-dependent symbiotic signalling and branching. *Nature* **483**: 341–344.

Lambers H. 2022. Phosphorus acquisition and utilization in plants. *Annual Review of Plant Biology* **73**: 17–42.

Lanfranco L, Fiorilli V, Venice F, Bonfante P. 2018. Strigolactones cross the kingdoms: plants, fungi, and bacteria in the arbuscular mycorrhizal symbiosis. *Journal of Experimental Botany* **69**: 2175–2188.

Li YL, Yang XY, Liu HJ, Wang W, Wang C, Ding GD, Xu FS, Wang SL, Cai HM, Hammond JP *et al.* 2022. Local and systemic responses conferring acclimation of roots to low phosphorus conditions. *Journal of Experimental Botany* **73**: 4753–4777.

Lin SI, Chiang SF, Lin WY, Chen JW, Tseng CY, Wu PC, Chiou TJ. 2008. Regulatory network of microRNA399 and *PHO2* by systemic signaling. *Plant Physiology* **147**: 732–746.

Liu N, Shen GJ, Xu YX, Liu H, Zhang JX, Li SL, Li J, Zhang CP, Qi JF, Wang L *et al.* 2020. Extensive inter-plant protein transfer between *Cuscuta* Parasites and their host plants. *Molecular Plant* **13**: 573–585.

López-Arredondo DL, Leyva-González MA, González-Morales SI, López-Bucio J, Herrera-Estrella L. 2014. Phosphate nutrition: improving low-phosphate tolerance in crops. *Annual Review of Plant Biology* **65**: 95–123.

Mohammed AE, Alotaibi MO, Elobeid M. 2022. Interactive influence of elevated CO_2 and arbuscular mycorrhizal fungi on sucrose and coumarin metabolism in *Ammi majus*. *Plant Physiology and Biochemistry* **185**: 45–54.

Müller LM, Harrison MJ. 2019. Phytohormones, miRNAs, and peptide signals integrate plant phosphorus status with arbuscular mycorrhizal symbiosis. *Current Opinion in Plant Biology* **50**: 132–139.

Nadal M, Sawers R, Naseem S, Bassin B, Kulicke C, Sharman A, An G, An K, Ahern KR, Romag A *et al.* 2017. An N-acetylglucosamine transporter required for arbuscular mycorrhizal symbioses in rice and maize. *Nature Plants* **3**: 17073.

Nagahashi G, Douds DD. 2011. The effects of hydroxy fatty acids on the hyphal branching of germinated spores of AM fungi. *Fungal Biology* **115**: 351–358.

Nanamori M, Shinano T, Wasaki J, Yamamura T, Rao IM, Osaki M. 2004. Low phosphorus tolerance mechanisms: phosphorus recycling and photosynthate partitioning in the tropical forage grass, *Brachiaria* hybrid cultivar Mulato compared with rice. *Plant and Cell Physiology* **45**: 460–469.

Nickrent DL. 2020. Parasitic angiosperms: how often and how many? *Taxon* **69**: 5–27.

Nussaume L, Kanno S, Javot H, Marin E, Pochon N, Ayadi A, Nakanishi TM, Thibaud MC. 2011. Phosphate import in plants: focus on the PHT1 transporters. *Frontiers in Plant Science* **2**: 83.

Pant BD, Buhtz A, Kehr J, Scheible WR. 2008. MicroRNA399 is a long-distance signal for the regulation of plant phosphate homeostasis. *The Plant Journal* **53**: 731–738.

Santoro V, Schiavon M, Visentin I, Constán-Aguilar C, Cardinale F, Celi L. 2021. Strigolactones affect phosphorus acquisition strategies in tomato plants. *Plant, Cell & Environment* **44**: 3628–3642.

Shahid S, Kim G, Johnson NR, Wafula E, Wang F, Coruh C, Bernal-Galeano V, Phifer T, dePamphilis CW, Westwood JH *et al.* 2018. MicroRNAs from the parasitic plant *Cuscuta campestris* target host messenger RNAs. *Nature* **553**: 82–85.

Shen GJ, Liu N, Zhang JX, Xu YX, Baldwin IT, Wu JQ. 2020. *Cuscuta australis* (dodder) parasite eavesdrops on the host plants' FT signals to flower. *Proceedings of the National Academy of Sciences, USA* **117**: 23125–23130.

Shen GJ, Zhang JX, Lei YT, Xu YX, Wu JQ. 2023. Between-plant signaling. *Annual Review of Plant Biology* **74**: 367–386.

Shi JC, Wang XL, Wang E. 2023. Mycorrhizal symbiosis in plant growth and stress adaptation: from genes to ecosystems. *Annual Review of Plant Biology* **74**: 569–607.

Shi JC, Zhao BY, Zheng S, Zhang XW, Wang XL, Dong WT, Xie QJ, Wang G, Xiao YP, Chen F *et al.* 2021. A phosphate starvation response-centered network regulates mycorrhizal symbiosis. *Cell* **184**: 5527–5540.

Siddiqi KS, Husen A. 2017. Plant response to strigolactones: current developments and emerging trends. *Applied Soil Ecology* **120**: 247–253.

Song J, Bian JG, Xue N, Xu YX, Wu JQ. 2022. Inter-species mRNA transfer among green peach aphids, dodder parasites, and cucumber host plants. *Plant Diversity* **44**: 1–10.

Stassen MJJ, Hsu SH, Pieterse CMJ, Stringlis IA. 2021. Coumarin communication along the microbiome-root-shoot axis. *Trends in Plant Science* **26**: 169–183.

Thibaud MC, Arrighi JF, Bayle V, Chiarenza S, Creff A, Bustos R, Paz-Ares J, Poirier Y, Nussaume L. 2010. Dissection of local and systemic transcriptional responses to phosphate starvation in Arabidopsis. *The Plant Journal* **64**: 775–789.

Varkonyi-Gasic E, Wu RM, Wood M, Walton EF, Hellens RP. 2007. Protocol: a highly sensitive RT-PCR method for detection and quantification of microRNAs. *Plant Methods* **3**: 12.

Wang L, Wang B, Yu H, Guo H, Lin T, Kou L, Wang A, Shao N, Ma H, Xiong G *et al.* 2020. Transcriptional regulation of strigolactone signalling in Arabidopsis. *Nature* **583**: 277–281.

Wang L, Zhang L, George TS, Feng G. 2022. A core microbiome in the hyphosphere of arbuscular mycorrhizal fungi has functional significance in organic phosphorus mineralization. *New Phytologist* **238**: 859–873.

Westwood JH, Yoder JI, Timko MP, dePamphilis CW. 2010. The evolution of parasitism in plants. *Trends in Plant Science* **15**: 227–235.

Yang SY, Lin WY, Hsiao YM, Chiou TJ. 2024. Milestones in understanding transport, sensing, and signaling of the plant nutrient phosphorus. *Plant Cell* **36**: 1504–1523.

Yoshida S, Cui SK, Ichihashi Y, Shirasu K. 2016. The Haustorium, a specialized invasive organ in parasitic plants. *Annual Review of Plant Biology* **67**: 643–667.

Yuan Y, Li J. 2022. Dodder parasitism limited the effect of arbuscular mycorrhizal fungi on litter decomposition. *Soil Biology and Biochemistry* **174**: 108837.

Zangishei Z, Annacondia ML, Gundlach H, Didriksen A, Bruckmüller J, Salari H, Krause K, Martinez G. 2022. Parasitic plant small RNA analyses unveil parasite-specific signatures of microRNA retention, loss, and gain. *Plant Physiology* **190**: 1242–1259.

Zhang JX, Li SL, Li WX, Feng ZR, Zhang SH, Zheng XJ, Xu YX, Shen GJ, Zhao M, Cao GY *et al.* 2024. Large-scale interplant exchange of macromolecules between soybean and dodder under nutrient stresses. *Plant Diversity* **46**: 116–125.

Zhang JX, Xu YX, Xie J, Zhuang HF, Liu H, Shen GJ, Wu JQ. 2021. Parasite dodder enables transfer of bidirectional systemic nitrogen signals between host plants. *Plant Physiology* **185**: 1395–1410.

Zhao B, Jia X, Yu N, Murray JD, Yi K, Wang E. 2023. Microbe-dependent and independent nitrogen and phosphate acquisition and regulation in plants. *New Phytologist* **242**: 1507–1522.

Supporting Information

Additional Supporting Information may be found online in the Supporting Information section at the end of the article.

Fig. S1 Effect of dodder parasitization on AMF colonization of tobacco plants.

Fig. S2 Effect of heterologous overexpression of Arabidopsis *IPS1* gene on tobacco phosphorus starvation response.

Fig. S3 Phenotypic characterization of oeIPS1.

Fig. S4 Relative expression levels of *IPS1* in dodder-connected plant clusters.

Fig. S5 Phenotypic characterization of tobacco *ccd8* mutants.

Fig. S6 Colonization of AMF and Pi content in tobacco *ccd8* mutants.

Fig. S7 Total P content and fresh and dry weights of plants in dodder-connected plant clusters.

Fig. S8 Heatmap indicating relative expression levels of the 63 upregulated genes.

Fig. S9 Heatmap indicating relative expression levels of the 38 downregulated genes.

Fig. S10 Analysis of SR plants' root transcriptomes in different plant clusters.

Fig. S11 Acid phosphatase activity and alkaline phosphatase activity in the rhizosphere soil of SR plants.

Fig. S12 KEGG terms with significant differences enriched from rhizosphere bacterial communities of SR plants of WT/oeIPS1 tobacco-dodder-WT tobacco clusters.

Fig. S13 Top 20 KEGG terms with significant differences enriched from rhizosphere bacterial communities of SR plants of WT/*ccd8* tobacco-dodder-WT tobacco clusters.

Methods S1 Supplemental methods.

Table S1 Primers used in this study.

Table S2 Recipe for modified Hoagland solution.

Table S3 All DEGs identified from the systemic signals receiver plants.

Table S4 Venn diagram analysis of DEGs in the systemic signals receiver plants.

Table S5 GO terms enriched from the genes, which were commonly up- and downregulated DEGs under +P condition but were not DEGs under −P condition.

Table S6 GO terms of biological process enriched from the specific DEGs in oeIPS1 vs WT.

Table S7 GO terms of biological process enriched from the specific DEGs in *ccd8* vs WT.

Table S8 Taxonomy of all OTUs in the rhizosphere bacterial communities of systemic signals receiver plants.

Table S9 Alpha diversity of the rhizosphere bacterial communities of systemic signals receiver plants.

Table S10 OTUs with relatively high abundance (not less than 10 sequences) of rhizosphere bacterial communities in each group of systemic signals receiver plants.

Table S11 Core OTUs in rhizosphere bacterial communities of systemic signals receiver plants.

Table S12 Mean relative abundance of the systemic signals receiver plants rhizosphere bacterial communities at phylum level.

Table S13 KEGG terms with significant differences enriched from rhizosphere bacterial communities of systemic signals receiver plants.

Table S14 Results of sequencing of miR399s in WT tobacco (SD)-dodder-WT tobacco (SR) clusters.

Please note: Wiley is not responsible for the content or functionality of any Supporting Information supplied by the authors. Any queries (other than missing material) should be directed to the *New Phytologist* Central Office.